CHEMISTRY
A European Journal

A Journal of
ChemPubSoc Europe

Accepted Article

Title: Potassium (De-)insertion Processes in Prussian Blue Particles: Ensemble versus Single Nanoparticle Behaviour

Authors: Giorgia Zampardi, Stanislav V. Sokolov, Christopher Batchelor-McAuley, and Richard G. Compton

To be cited as: *Chem. Eur. J.* 10.1002/chem.201703175

Link to VoR: http://dx.doi.org/10.1002/chem.201703175

Supported by
ACES

WILEY-VCH

10.1002/chem.201703175

WILEY-VCH

Potassium (De-)insertion Processes in Prussian Blue Particles: Ensemble versus Single Nanoparticle Behaviour

Giorgia Zampardi[a], Stanislav V. Sokolov[a], Christopher Batchelor-McAuley[a] and Richard G. Compton*[a]

Abstract: Potassium (de-)insertion from Prussian Blue (PB) is investigated at the single and multi-particle scale. The electrochemical behaviour is found to differ between the two measurement types. At the single particle level oxidation of the PB nanoparticles with concomitant K^+ deinsertion occurs more readily than the associated reduction, relating to K^+ insertion. In contrast, the cyclic voltammetry of PB in a composite electrode containing conductive additives and polymeric binder suggests the opposite behaviour. Implications for assessing battery materials are discussed.

Introduction

Although lithium-ion batteries are undisputedly successful within the portable electronics and electric-powered vehicles markets, in the frame of large-scale power grid applications their use is strongly limited due to high costs, toxicity and uneven distribution of lithium resources [1]. Consequently, in the last two decades research has focused on different metal-ion systems in aqueous electrolytes for the production of cheaper, safer and more environmentally friendly alternatives to lithium-ion batteries, which would fit the specifications required for large scale stationary applications. Metal-ion battery systems alternative to the Li-ion technology are based on Na-, Zn-, and K-ion chemistries even if for them to be commercialised their energy densities, power densities and cycle lives have still to be increased and electrode materials optimised[2] [3] [3b].

Because of the usually poor electronic conductivity of the active materials, the conventional fabrication and analysis employed for metal-ion battery systems is based almost exclusively on the use of porous composite electrodes made of a mixture of the active material, conductive additives (often carbon particles) and a polymeric binder (polyvinylidene difluoride for example). The presence of the usually insulating polymeric binder improves greatly the mechanical stability of the electrode by holding the particles together, whilst the conductive additive decreases the intra-particle resistance, so modifying the electron transfer process within the porous composite electrode. In order to overcome the limitations posed by the use of such porous composite electrodes, research has focused lately on the engineering of nanostructured materials within the energy storage field with the aim of decreasing the overall weight of the electrodes and its inactive components in order to increase the energy density of the battery system [4]. Moreover, the use of nanostructured electrodes has the advantage of decreasing the resistance in terms of optimising the electron and ion transfer to/from the active material interface leading to an increase in the power density of the battery system [4]. In order to achieve a better engineering of the nanostructured systems and high efficiencies at the nanoscale, it is important to understand the intrinsic behaviour of such materials at the nanoparticle level, without the influence of conductive additives and binders on the electrochemical response of the active components. To this extent it is of fundamental importance to understand if and how the behaviour of such materials changes between the ensemble level and the single particle level.

Among the materials used for metal-ion batteries, hexacyano metallates and in particular iron hexacyanoferrate and its analogues have recently attracted significant interest since they are promising insertion materials for K-ion [5], Zn-ion [2, 6] and Na-ion [7] batteries. Prussian Blue, or iron(III) hexacyanoferrate(II), is the predecessor of this class of materials and has been widely studied as a paradigm case because of its stable and reversible K-insertion electrochemistry at room temperature in aqueous based electrolytes. Its diverse applications range from K-ion batteries[5a, 5b], chemical and biological sensors [8], H_2O_2 catalysis [9] and electrochromic devices [10].

In this study the electrochemical behaviour of single Prussian Blue nanoparticles is investigated and compared to the ensemble response. Single nanoparticle analysis was performed through the electrode-particle impact method in which particles are suspended in solution and they may, by virtue of their Brownian motion, collide with a potentiostated microelectrode. The stochastic collisions result in spikes in the background current recorded at the microelectrode[11]. The magnitude of the charge, duration and frequency of a numerically relevant number of single collision events, leads to direct information regarding the reactions occurring at the nanoscale [12]. Electrode-particle impacts are an effective technique that facilitates the study of solution phase behaviour and reactivity of *individual* particles. Impact techniques have been applied to a diverse range of systems from small (d = 8 nm) silver nanoparticles [13] to complex living cells [14]. Bard et al. demonstrated how the technique can be used to study catalytic activity of single Pt nanoparticles by monitoring proton reduction reaction taking place upon the collision of the particle with an inert electrode. [15] [16] The application of electrode-particle impacts to energy related materials was first investigated by the observation of impacts of $LiMn_2O_4$ particles and the current transients due to Li^+ deinsertion from the material at the single particle level [17]. The work was followed by a report of Sun et al. who studied the oxidation of $LiCoO_2$ particles through electrode-particle collisions and correlated imaging and electrochemical recording [18]. As in the case of $LiMn_2O_4$ particles [17] the investigation of the intrinsic electrochemical behaviour of the material can be focused only on one process, i.e. Li^+ deinsertion, because of the very nature of the collision experiments which prevents the particle to be cycled allowing the study of a process only in one direction. The

[a] Dr. G. Zampardi, S. V. Sokolov, Dr. C. Batchelor-McAuley, Prof. Dr. R. G. Compton
Department of Chemistry, Physical and Theoretical Chemistry Laboratory (PTCL)
University of Oxford
South Parks Road, OX1 3QZ, Oxford, United Kingdom
E-mail: richard.compton@chem.ox.ac.uk

Supporting information for this article is given via a link at the end of the document.

main interest offered by using Prussian Blue particles is that having already potassium ions within their structure (that can be deinserted) and being able to accommodate a second one (that can be inserted), the use of these particles with the nano-impact method opens up the possibility to study both the cation insertion and deinsertion on the same particle. For this reason the electrochemical behaviour of the material towards K^+ (de-)insertion was investigated at the single particle level and the results compared to the behaviour of the material at the ensemble level which is influenced by the presence of binder and conductive additive particles.

Results and Discussion

Prussian Blue, or iron(III) hexacyanoferrate(II), i.e. $KFe^{III}[Fe^{II}(CN)_6]$, has a face centred cubic structure with low spin iron(III) and high spin iron(II) surrounded octahedrically by nitrogen atoms and carbon atoms respectively [19]. To ensure the lattice electroneutrality, potassium ions and/or Fe^{3+} ions are located in interstitial positions within the crystal structure with a stoichiometry which is dependent on the synthesis route of the material [20]. In the literature, the older terminology "soluble" and "insoluble" Prussian Blue remain widely used to indicate $KFe^{III}[Fe^{II}(CN)_6]$ and $Fe^{II}_4[Fe^{III}(CN)_6]_3$, respectively however it is important to recognise that both these forms are in fact essentially insoluble, and the term "soluble" relates to the ability of the material to form a stable colloidal suspension[8a, 9a]. Moreover, upon electrochemical polarisation of a Prussian Blue immobilised electrode in aqueous solutions containing potassium cations, "insoluble" Prussian Blue undergoes structural changes that give "soluble" Prussian Blue as a result of its oxidation (interstitial Fe^{3+} release) followed by its reduction (interstitial K^+ intake). Indeed, there are several studies that demonstrate the stability of such compounds once deposited on various electrodes to be independent of the level of potassium present within the interstitial sites of the lattice [5b, 8a, 9a, 20b, 21].

$$KFe^{III}[Fe^{II}(CN)_6] \underset{-K^+ - e^-}{\overset{+K^+ + e^-}{\rightleftharpoons}} K_2Fe^{II}[Fe^{II}(CN)_6] \quad \text{Eq. 1}$$

Prussian Blue — Prussian White, Berlin White, Everitts Salt

$$KFe^{III}[Fe^{II}(CN)_6] \underset{+K^+ + e^-}{\overset{-K^+ - e^-}{\rightleftharpoons}} Fe^{III}[Fe^{III}(CN)_6] \quad \text{Eq. 2}$$

Prussian Blue — Prussian Yellow, Berlin Green

Among all the hexacyanoferrate-based materials, Prussian Blue (PB) has been widely studied as a model system for insertion electrochemistry since it can easily insert potassium cations maintaining high reversibility and high stability during its cycling [5a, 5b, 20b]. Upon the electrochemical reduction of low spin iron(III), K^+ ions are inserted into the crystal structure concomitantly to the electron transfer in order to maintain the electroneutrality of the lattice, thus forming $K_2Fe^{II}[Fe^{II}(CN)_6]$ (Eq.1). Because of the colour change of the material during this reaction from dark blue to white, the resulting compound was called Prussian White (PW), or Berlin White (BW), or Everitts Salt (ES). Upon electrochemical oxidation of the high spin iron(II), K^+ ions are deinserted from the interstitial positions of the PB crystal structure forming $Fe^{III}[Fe^{III}(CN)_6]$ (Eq.2). This reaction is followed by a colour change from deep blue to green, upon partial oxidation, or to yellow, upon full oxidation. For this reason, the resulting compound was called Berlin Green (BG) or Prussian Yellow (PY), depending on the extent of its oxidation degree.

In order to study the voltammetric response of Prussian Blue nanoparticles as an ensemble, a glassy carbon electrode with a diameter of 3.0 mm was modified with c.a. 0.4 mg of a slurry made of Prussian Blue nanoparticles, conductive carbon additive and PVdF polymeric binder, in a weight ratio of 80:10:10 Experiments performed through dropcasting pure Prussian Blue nanoparticles onto a glassy carbon electrode are not reported since they showed variable voltammetric behaviours, most likely due to different degrees of agglomeration of the PB nanoparticles on the electrode surface[22]. Initially the composite electrode was swept cathodically at a scanrate of 0.1 mV s^{-1} in order to reduce Prussian Blue to Prussian White with the consequent K^+ insertion within its crystal lattice (Fig.1). The cyclic voltammogram of the composite Prussian Blue based electrode is characterised by two distinct sets of peaks related to the two redox centres: low spin iron(III) nitrogen-coordinated and high spin iron(II) carbon-coordinated [8a, 9a, 20b].

The set of peaks between 0.15 and 0.3 V vs. SCE, are related to equation (1) and suggest that such reaction occurs rapidly on the time scale of the voltammetry within the composite electrode [9a]. When the applied potential reaches more anodic values between 0.85 and 0.95 V vs. SCE, PB is converted to its oxidised state Berlin Green or Prussian Yellow (when the PB oxidation is complete), with the concomitant deinsertion of K^+ from the PB lattice. This second set of peaks is much broader in comparison to peaks A and B. This could possibly indicate that the reaction is limited by the diffusion of K^+ to/from the particle. Further evidence for this diffusional limitation is that only c.a. 30% of the PB present in the composite electrode has reacted. In contrast the cathodic peaks set shows that nearly 100% of PB was converted into PW (and vice versa).

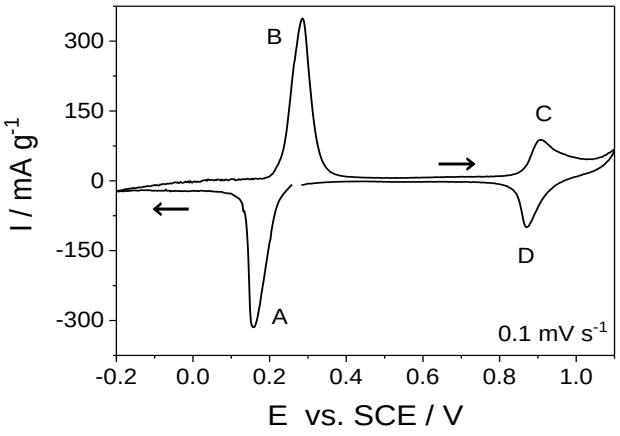

Figure 1. Cyclic voltammogram of a prussian blue based paste electrode in a solution containing KCl 1 M at a scan rate of 0.1 mV s^{-1}. Starting potential of the voltammetry: 0.3 V. The current is normalised per gram of active material ($KFe^{III}[Fe^{II}(CN)_6]$). Peak potentials: (A) 0.15 V, (B) 0.28 V, (C) 0.91 V, (D) 0.87 V vs. SCE.

It is worth mentioning that the high mechanical stability of the composite electrode made the results highly reproducible probably because of the presence of the PVdF binder, ruling out the possibility of active material particles becoming detached during the experiment.

The cyclic voltammetry shown in Fig. 1 was recorded at a very low scan rate of 0.1 mV s^{-1} in order to minimise any cation diffusion limitations in both the solid and the liquid phases [23] which arise from the porous nature of the electrode. This attempts to ensure that the electrochemical behaviour of the porous electrode did not originate from the nature and the geometry of the composite matrix itself, but on the PB contained in it. In fact, when the scan rate is increased (SI section 1) there is a shift in the peaks potential of several hundreds of millivolts and both peaks A-B and C-D appear diffusion limited in the solid phase[20b, 23a]. This is further confirmed by the analysis of the peak current of both peak sets A-B and C-D in dependence of the scan rate (SI section 1), in accordance with that previously reported [20b].

Subsequent to the ensemble measurements the electrochemical behaviour of *single* PB nanoparticles was analysed by dispersing them in solution and holding a carbon microdisc electrode at a suitable potential. During the chronoamperogram when 3.5 pM of PB particles (SI section 2) were present in solution, clear spikes in the baseline current were observed, as shown in Fig.2. Such spikes relate to the stochastic arrival of PB nanoparticles at the electrode surface and their reaction involving K^+ deinsertion from its lattice.

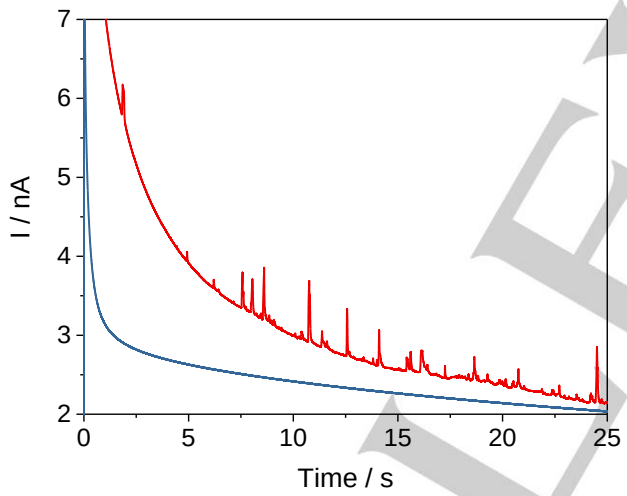

Figure 2. Chronoamperogram of a carbon disc microelectrode in a solution containing 10 mM KCl with (red line) and without (blue line) Prussian Blue nanoparticles 3.5 pM. Electrode polarised at 1.4 V SCE.

Oxidative spikes were observed in solutions containing 0 mM, 1 mM and 10 mM KCl and when the carbon microdisc electrode was polarised at 1.4 V vs. SCE. In all cases it was required an overall overpotential of c.a. 350 mV, relative to the formal potential of the reaction involving PB and PY/BG (Eq. 1) which was estimated to be 0.93 V vs. SCE from the midpeak potential of the cyclic voltammetry of the ensemble shown in Fig.1, in accordance to the literature[24].

From Fig.3a the average charge of the oxidative spikes was found to be 4.5 ± 3.3 pC and nearly independent of the electrolyte concentration. From the particle light scattering analysis (SI section 2) the average diameter of the particles in solution was estimated to be 190 ± 85 nm. The oxidation of such an average nanoparticle would require an estimated 3 ± 2.8 pC, indicating that the nanoparticles are completely oxidised upon collision with the carbon microelectrode, assuming one electron transferred per every K^+ inserted. The average impact frequency is shown in Fig.3b and it was found to be constant with the KCl concentration. From the Stokes-Einstein equation considering the average particle diameter, the average diffusion coefficient of a single PB nanoparticle is calculated to be c.a. 2.6 × 10^{-12} m^2 s^{-1}. Using the average diffusion coefficient and an integrated form of the Shoup-Szabo Equation the average impact frequency can be predicted to be c.a. 1 s^{-1}. From Fig.3b the spikes frequency experimentally determined is roughly consistent with the theoretical estimated value, which considers a diffusion-only mass transport of the particles and neglects hindered diffusion processes in the very close proximity to the interface [25].

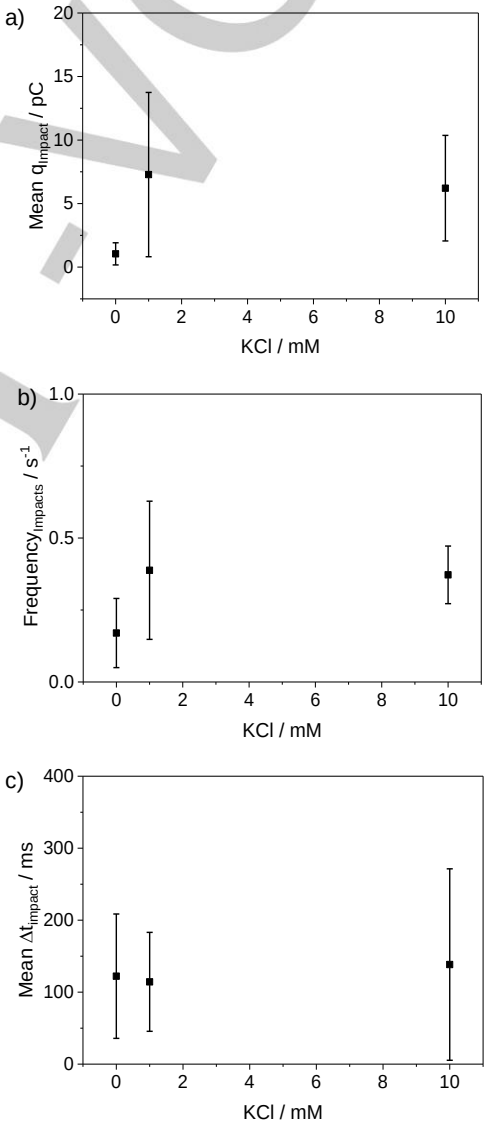

Figure 3. a) Mean charge, b) mean frequency and c) mean duration of the PB particle impacts (error bas represent the interquartile range) recorded in different KCl concentrations. Carbon microelectrode polarised at 1.4 V vs. SCE. The impact frequencies were normalised per chronoamperogram (25 s) recorded.

The average duration of the oxidative events shown in Fig.3c was found to be 125 ± 12 ms. It is worth to commenting that, despite reports of self-assembled Prussian Blue layers formed

chemically or electrochemically onto electrode surfaces as gold, ITO, etc. [26], after the chronoamperograms performed for the nano-impact experiments no PB layer was found on the microelectrode surface immersed in the PB suspension independently of the potential applied to the microelectrode, as shown in SI section 3.

Interestingly no reductive spikes related to K^+ insertion into the PB nanoparticle were observed in any electrolyte solution tested (1 mM, 10 mM, 50 mM or 100 mM KCl), regardless of the potential applied to the carbon microdisc electrode, ranging from 0.1 to -1.4 V vs. SCE. Measurements at higher KCl concentrations were attempted but lead to an obvious agglomeration of the nanoparticles suspension. However, even at a low 1 mM KCl concentration, the K^+ insertion within the PB nanoparticle is unlikely to be limited by the K^+ diffusion in the aqueous phase. For an average nanoparticle with a diameter of 190 nm, 9.7×10^{-16} g of K^+ are required for its complete reduction (or oxidation). Given 5 mL of solution with a concentration of 1 mM KCl and a diffusion coefficient of K^+ ions in aqueous solution of 1.9×10^{-5} cm^2 s^{-1} [27], the diffusion time (r^2/D_{K+})[28] of K^+ ions in the liquid phase was estimated to be around 2 ms. This means that if the K^+ insertion upon a collision event were limited by the K^+ diffusion at the liquid phase, its duration would be at least of 2 ms. Considering the response of the potentiostat employed for this study, spikes having a duration of this order of magnitude can be distinguished from the background noise, even if their shape can be modified by the response of the potentiostat[29]. For this reason it can be concluded that the redox processes occurring during the impact event are not limited by the diffusion of K^+ ions in solution, even at low K^+ concentrations. This suggests that either reductive collision events do not occur in this potential range, or the K^+ insertion kinetics at the single particle level occurs at longer times than the collision time scale, making their detection not to be distinguishable from the background noise [29].

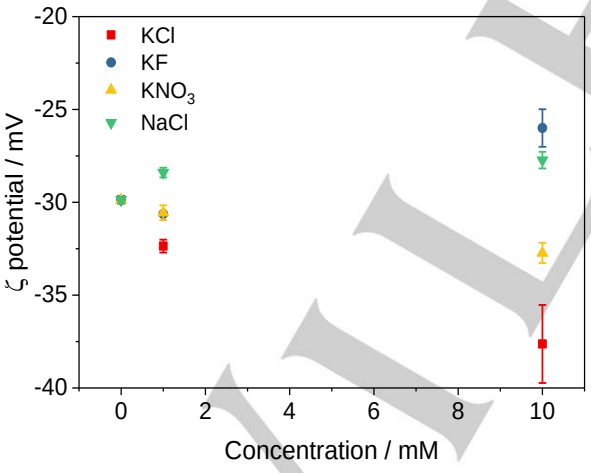

Figure 4. Zeta potential of Prussian Blue nanoparticles measured from a solution containing 3.5 pM PB NPs and different salt in dependence of the electrolyte concentrations.

The fact that no reductive spikes were observed during the impact experiments may at least in principle relate to possible electrostatic repulsion between the impacting PB nanoparticles and the carbon microelectrode surface, inhibiting the electrical contact between them. The Zeta potential of PB nanoparticles suspended in pure water and in different solutions with different salts was measured as a function of the electrolyte concentration (Fig.4), and was found to be negative for all cases. All zeta potential values were below -20 mV indicating moderate stability of the suspended particles. [30]

The potential of zero charge (PZC) of the carbon microdisc electrode was estimated by means of the microelectrode capacitance at different applied potentials. The microelectrode capacitance was calculated through cyclic voltammetries performed over a restricted potential range of 100 mV at a high scan rate of 2 V s^{-1} (SI section 4), as previously reported [31].

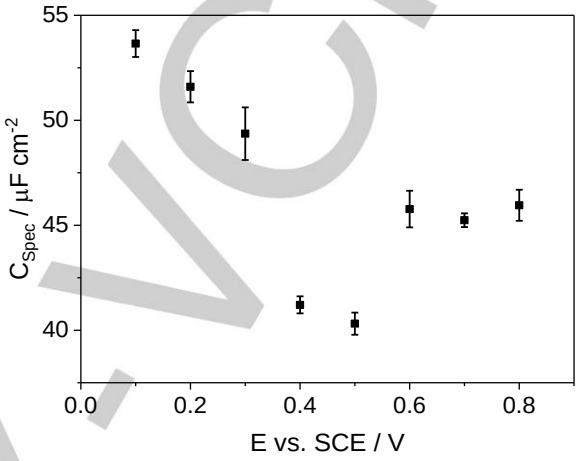

Figure 5. Variation of the specific capacitance of the carbon fibre microdisc electrode as a function of potential. The capacitance was measured via cyclic voltammetry in a solution containing 1.0 mM KCl. The minimum indicates the position of the point of zero charge of the microdisc electrode.

Fig.5 shows a minimum in the measured electrode capacitance at around 0.45 mV vs. SCE, which likely corresponds approximately to the PZC of the carbon microelectrode. Since the K^+ insertion into PB nanoparticles requires potentials applied to the microelectrode equal or lower than 0.1 V vs. SCE (as shown in Fig.1), the surface of the latter will be negatively charged and could electrostatically hinder the nanoparticle-electrode collisions. However electrostatic repulsion effects are usually negligible within the range of electrolyte concentration used for the impact experiments [11a]. It was demonstrated for negatively charged indigo nanoparticles that destructive impacts (i.e. when the particles undergo a complete dissolution upon collision) occurred independently of the surface charge of the electrode, which was polarised positively and negatively with the respect of its potential of zero charge [32]. Prussian Blue nanoparticle collisions are not destructive in nature, since K^+ (de-)insertion processes do not lead to the dissolution of the nanoparticle itself upon collision, and electrostatic effects may be occurring at 1 mM KCl. However at 10 mM this effect would be expected to be already negligible because of the charge screening by the electrolyte. Moreover for the case of the indigo NPs repulsive electrostatic effects were not observed for electrolyte concentrations as low as 5 mM KCl [32]. Moreover, if the electrostatic repulsion in the diffusion layer were to hinder the nanoparticle-electrode collisions, reductive events should have been observed at higher electrolyte concentrations. The fact that no reductive collisions were observed with any of the electrolyte concentrations tested can therefore more reasonably be ascribed to a slower K^+

insertion kinetics (with the respect to the K^+ insertion) at the single nanoparticle level. In this case, the material behaviour changes qualitatively from the ensemble level to the nanoparticle level.

Conclusions

The nanoimpact method was applied to the study of the intrinsic K^+ (de-)insertion processes in single Prussian Blue particles. This analysis offered the possibility of investigating the material behaviour without the influence of conductive additives and polymeric binder, which are needed since composite electrodes are routinely used for battery materials analysis and Prussian Blue is one of the most effective materials for K^+ (de-)insertion in K-ion batteries[5a, 5b]. Here the electrochemical behaviour of Prussian Blue particles was compared to the one at the composite ensemble level. As an ensemble, the K^+ insertion into Prussian Blue (which is converted to Prussian White) appears kinetically favoured, while only 30% of the material participates into the K^+ deinsertion (Prussian Blue converted to Berlin Green), which appears sluggish and diffusion limited despite the slow scan rate of the voltammetry.

However, at the single nanoparticle level only oxidative events were observed (K^+ deinsertion from PB, which turns into Berlin Green/Prussian Yellow) in all the conditions tested. The fact that no reductive collision events appeared could be related to an electrostatic repulsion between the negatively charged PB particles and the electrode surface, which is always negatively charged for potentials lower than 0.45 V SCE (from the estimation of the potential of zero charge of the carbon microelectrode). The electrostatic repulsion is strongly dependent on the ionic strength of the solution and on the surface charge of the nanoparticle.

Electrostatic effects were demonstrated not to affect the collision of negatively charged indigo NPs towards a negatively charged electrode [32]. Moreover, if the electrostatic repulsion hindered the approach of the PB nanoparticle towards the electrode at a distance where the electron transfer could occur, reductive events should have been visible at electrolyte concentrations above 10 mM KCl [32]. For this reason the fact that no reduction of the PB particles occurred at the nanoscale is likely attributable to slower K^+ insertion kinetics which could not be resolved in the time scale of the collision experiments. The electrochemical behaviour of the material at the nanoscale differs from that suggested from the cyclic voltammentry of the ensemble electrode. This striking difference suggests that when nanomaterials and nanostructured materials are employed for energy storage application, it is important to study the direct behaviour of the active materials both with and without the influence of conductive additives and binders. Conductive additives and binders routinely used for the conventional battery analysis play indeed a non-passive role, since they influence the electrochemical response of the composite electrodes [33]. The nano-impact methods was proven to be an effective way to test the intrinsic electrochemical behaviour at the nanoscale and to give important and alternative insight to the conventional analysis usually performed on these systems, opening up new possibilities for the engineering of nanoscale materials and the optimisation of their working conditions.

Experimental Section

Materials

Prussian Blue or iron(III) hexacyanoferrate(II) (KFeII[FeIII(CN)6]) nanoparticles were purchased from Sigma Aldrich UK. Potassium Chloride, Potassium Fluoride, Potassium Nitrate and Sodium Chloride were obtained from Sigma Aldrich UK and used as received. All solutions were prepared using ultrapure water (Millipore), with a resistivity of 18.2 MΩ cm at 298 K.

Cyclic voltammetry experiments on composite electrodes

All cyclic voltammetry was performed in a three electrode electrochemical cell using an Autolab III (Methrom Autolab B.V., The Netherlands). For the Prussian Blue cyclic voltammetries the working electrode consisted of a $KFe^{III}[Fe^{II}(CN)_6]$ slurry drop cast onto a glassy carbon electrode with a diameter of 3 mm (ALS, Japan). The starting slurry was made of a mixture of $KFe^{III}Fe^{II}(CN)_6]$ particles, polyvinylidene fluoride binder (PVdF Solef S5130, Solvay, Belgium) and conductive carbon additive Super C65 (Timcal, Switzerland) in N-methylpyrrolidone (NMP, Sigma Aldrich, UK), with a weight ratio of 80:10:10. The resulting slurry was stirred overnight with a magnetic stirrer and ca. 0.4 mg were dropcast onto a glassy carbon electrode surface. The modifying porous [17]layer had a thickness of approximately 10 μm. All the electrodes were heated at ca. 60˚C for 1h in order to evaporate the NMP solvent. Pt foil (Goodfellow, UK) was employed as a counter electrode and a saturated calomel electrode (SCE, +0.241 V vs SHE) (ALS, Japan) was used as a reference electrode.

Specific capacitance and nanoimpact experiments

Cyclic voltammetry experiments performed to calculate the specific capacitance of a carbon microelectrode and all the nano-impact experiments were performed in a three electrode electrochemical cell put inside a double Faraday cage. An in-house built low noise potentiostat was used with a 100 Hz Bessel-type low pass filter [13]. The analog-to-digital and digital-to-analog conversion was provided by a USB-6003 DAQ (National Instruments, Tx, USA). The control of these devices were performed by a script written in Python 2.7 with a graphical user interface and real-time electrochemical data visualization based upon the packages provided in the Enthought Tool Suite (Enthought, TX, USA). When the system was used for electrode-particle collision experiments, the charge passed during an impact event is conserved although the current-time response may, at short times, be distorted [29]. The working electrode was a carbon microdisk electrode with a 33 μm diameter (ASL, Japan). Pt foil and saturated calomel electrodes were used as the reference and counter electrodes.

Prussian Blue nanoparticles characterisation

Zeta potential measurements were performed using Malvern Zetasizer Nano ZS system with an irradiation wavelength of 632.8 nm He laser. Disposable folded capillary cells were filled with the solution to be analysed and measured.

Nanoparticle Tracking Analysis (NTA) was performed through a NanoSight LM10 (NanoSight, UK), equipped with a sample chamber with a 638 nm laser. The samples were injected in the sample chamber with sterile syringes (BsD Discardit II, New Jersey, USA), ensuring the absence of any air bubbles. All measurements were performed at a temperature of 25˚C. The samples were measured for 60 s with automatic exposure settings at 30 frames per second. The software used for video capture and data analysis was the NTA 2.3.

Dynamic light scattering (DLS) measurements were performed using Malvern Zetasizer Nano ZS system with an irradiation wavelength of 632.8 nm He laser. The measurement was repeated three times to estimate the associated error. For data processing a general purpose (normal resolution) algorithm was used.

Scanning electron microscopy (SEM) imaging was performed by JEOL JSM-6500F Scanning Electron Microscope with an accelerating voltage of 5 kV using secondary electron imaging mode. Sample preparation involved the dropcast of Prussian Blue particles on a conductive glassy carbon substrate followed by drying under nitrogen atmosphere. Fig. 6 shows the image of the Prussian Blue nanoparticles. Significant clustering is observed which is likely due to the aggregation/agglomeration upon drying.

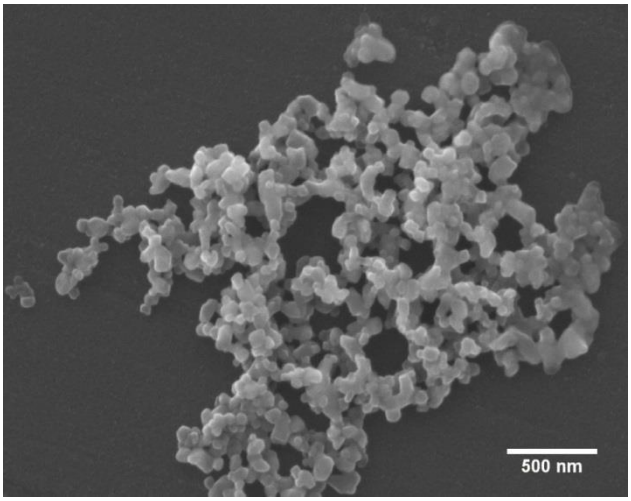

Figure 6. SEM image of Prussian Blue nanoparticle onto a glassy carbon substrate.

Acknowledgements

The research leading to these results has received fundings from the European Research Council under the European Union's Seventh Framework Program (FP/2007-2013)/ERC Grant Agreement No. 320403

Keywords: (De-)insertion Kinetics • Potassium-ion Batteries • Potential of Zero Charge • Prussian Blue • Single Nanoparticle Electrochemistry

[1] aR. Trocoli, A. Battistel, F. La Mantia, *Chem.-Eur. J.* **2014**, *20*, 9888-9891; bR. Trocoli, A. Battistel, F. La Mantia, *ChemSusChem* **2015**, *8*, 2514-2519; cR. Trocoli, C. Erinmwingbovo, F. La Mantia, *ChemElectroChem* **2017**, *4*, 143-149.

[2] G. Kasiri, R. Trocoli, A. B. Hashemi, F. La Mantia, *Electrochim. Acta* **2016**, *222*, 74-83.

[3] aK. Kubota, S. Komaba, *Journal of The Electrochemical Society* **2015**, *162*, A2538-A2550; bM. Sawicki, L. L. Shaw, *RSC Adv.* **2015**, *5*, 53129-53154.

[4] Q. Zhang, E. Uchaker, S. L. Candelaria, G. Cao, *Chem Soc Rev* **2013**, *42*, 3127-3171.

[5] aM. Jayalakshmi, F. Scholz, *J. Power Sources* **2000**, *91*, 217-223; bM. Jayalakshmi, F. Scholz, *J. Power Sources* **2000**, *87*, 212-217; cK. Honda, *Journal of The Electrochemical Society* **1987**, *134*, 1330;

[6] R. Trocoli, F. La Mantia, *ChemSusChem* **2015**, *8*, 481-485.

[7] aC. D. Wessells, S. V. Peddada, M. T. McDowell, R. A. Huggins, Y. Cui, *Journal of the Electrochemical Society* **2012**, *159*, A98-A103; bC. D. Wessells, S. V. Peddada, R. A. Huggins, Y. Cui, *Nano Lett* **2011**, *11*, 5421-5425; cM. Pasta, R. Y. Wang, R. Ruffo, R. Qiao, H.-W. Lee, B. Shyam, M. Guo, Y. Wang, L. A. Wray, W. Yang, M. F. Toney, Y. Cui, *J. Mater. Chem. A* **2016**, *4*, 4211-4223.

[8] aA. A. Karyakin, E. E. Karyakina, *Russ. Chem. Bull.* **2001**, *50*, 1811-1817; bE. E. Karyakina, A. V. Lukhnovich, E. I. Yashina, M. A. Statkus, G. I. Tsisin, A. A. Karyakin, *Electroanalysis* **2016**, *28*, 2389-2393; cA. V. Mokrushina, M. Heim, E. E. Karyakina, A. Kuhn, A. A. Karyakin, *Electrochem. Commun.* **2013**, *29*, 78-80; dE. A. Puganova, A. A. Karyakin, *Sens. Actuator B-Chem.* **2005**, *109*, 167-170; eA. Karyakin, **2008**, 411-439; fA. A. Karyakin E. A. Puganova, I. A. Bolshakov, E. E. Karyakina, *Angew Chem Int Ed Engl* **2007** *46*, 7678-7680.

[9] aA. A. Karyakin, *Electroanalysis* **2001**, *13*, 813-819; bN. A. Sitnikova, M. A. Komkova, I. V. Khomyakova, E. E. Karyakina, A. A. Karyakin, *Anal. Chem.* **2014**, *86*, 4131-4134.

[10] L. M. N. Assis, R. Leones, J. Kanicki, A. Pawlicka, M. M. Silva, *J. Electroanal. Chem.* **2016**, *777*, 33-39.

[11] aS. V. Sokolov, S. Eloul, E. Katelhon, C. Batchelor-McAuley, R. G. Compton, *Phys. Chem. Chem. Phys.* **2017**, *19*, 28-43; bW. Cheng, R. G. Compton, *TrAC Trends in Analytical Chemistry* **2014**, *58*, 79-89; cY. G. Zhou, B. Haddou, N. V. Rees, R. G. Compton, *Phys Chem Chem Phys* **2012**, *14*, 14354-14357.

[12] E. Kätelhön, A. Feng, W. Cheng, S. Eloul, C. Batchelor-McAuley, R. G. Compton,

The Journal of Physical Chemistry C **2016**, *120*, 17029-17034.

[13] C. Batchelor-McAuley, J. Ellison, K. Tschulik, P. L. Hurst, R. Boldt, R. G. Compton, *Analyst* **2015**, *140*, 5048-5054.

[14] L. Sepunaru, S. V. Sokolov, J. Holter, N. P. Young, R. G. Compton, *Angew Chem Int Ed Engl* **2016**, *55*, 9768-9771.

[15] X. Xiao, A. J. Bard, *J Am Chem Soc* **2007**, *129*, 9610-9612.

[16] X. Xiao, F. R. Fan, J. Zhou, A. J. Bard, *J Am Chem Soc* **2008**, *130*, 16669-16677.

[17] G. Zampardi, C. Batchelor-McAuley, E. Katelhon, R. G. Compton, *Angew Chem Int Ed Engl* **2017**, *56*, 641-644.

[18] L. L. Sun, D. Jiang, M. Li, T. Liu, L. Yuan, W. Wang, H. Y. Chen, *Anal. Chem.* **2017**, *89*, 6051-6056.

[19] K. Itaya, I. Uchida, V. D. Neff, *Accounts Chem. Res.* **1986**, *19*, 162-168.

[20] aA. Dostal, B. Meyer, F. Scholz, U. Schroder, A. M. Bond, F. Marken, S. J. Shaw, *J. Phys. Chem.* **1995**, *99*, 2096-2103; bN. F. Zakharchuk, B. Meyer, H. Hennig, F. Scholz, A. Jaworksi, Z. Stojek, *J. Electroanal. Chem.* **1995**, *398*, 23-35.

[21] F. Ricci, G. Palleschi, *Biosens Bioelectron* **2005**, *21*, 389-407.

[22] aS. J. Cloake, H. S. Toh, P. T. Lee, C. Salter, C. Johnston, R. G. Compton, *ChemistryOpen* **2015**, *4*, 22-26; bH. S. Toh, C. Batchelor-McAuley, K. Tschulik, M. Uhlemann, A. Crossley, R. G. Compton, *Nanoscale* **2013**, *5*, 4884-4893; cK. Tschulik, C. Batchelor-McAuley, H. S. Toh, E. J. Stuart, R. G. Compton, *Phys Chem Chem Phys* **2014**, *16*, 616-623.

[23] aD. Aurbach, M. D. Levi, E. Levi, H. Teller, B. Markovsky, G. Salitra, U. Heider, L. Heider, *Journal of the Electrochemical Society* **1998**, *145*, 3024-3034; bF. Scholz, B. Meyer, *Chem Soc Rev* **1994**, *23*, 341-347.

[24] aM. B. Soto, F. Scholz, *J. Electroanal. Chem.* **2002**, *521*, 183-189; bF. Scholz, A. Dostal, *Angewandte Chemie International Edition in English* **1996**, *34*, 2685-2687.

[25] aS. Eloul, R. G. Compton, *J Phys Chem Lett* **2016**, *7*, 4317-4321; bS. Eloul, E. Kätelhön, C. Batchelor-McAuley, K. Tschulik, R. G. Compton, *J. Electroanal. Chem.* **2015**, *755*, 136-142; cS. Eloul, E. Katelhon, R. G. Compton, *Phys Chem Chem Phys* **2016**, *18*, 26539-26549.

[26] aR. Cisternas, E. Munoz, R. Henriquez, R. Cordova, H. Kahlert, U. Hasse, F. Scholz, *J. Solid State Electrochem.* **2011**, *15*, 2461-2468; bA. Jaiswal, J. Colins, B. Agricole, P. Delhaes, S. Ravaine, *J Colloid Interface Sci* **2003**, *261*, 330-335; cM. Pyrasch, A. Toutianoush, W. Q. Jin, J. Schnepf, B. Tieke, *Chem. Mat.* **2003**, *15*, 245-254.

[27] H. S. Harned, R. L. Nuttall, *Journal of the American Chemical Society* **1947**, *69*, 736-740.

[28] A. Einstein, *Annalen der Physik* **1905**, *322*, 891-921.

[29] E. Kätelhön, E. E. L. Tanner, C. Batchelor-McAuley, R. G. Compton, *Electrochim. Acta* **2016**, *199*, 297-304.

[30] R. H. O. a. R. L. R. Robert J. Hunter, *Zeta Potential in Colloid Science: Principles and Applications*, Elsevier **1981**.

[31] R. Nissim, C. Batchelor-McAuley, M. C. Henstridge, R. G. Compton, *Chem Commun (Camb)* **2012**, *48*, 3294-3296.

[32] K. Tschulik, W. Cheng, C. Batchelor-McAuley, S. Murphy, D. Omanović, R. G. Compton, *ChemElectroChem* **2015**, *2*, 112-118.

[33] L. Fransson, T. Eriksson, K. Edström, T. Gustafsson, J. O. Thomas, *J. Power Sources* **2001**, *101*, 1-9.

10.1002/chem.201703175

WILEY-VCH

Entry for the Table of Contents (Please choose one layout)

Layout 1:

FULL PAPER

Potassium insertion and deinsertion processes were investigated in Prussian Blue at the nanoscale through the nanoimpact method. The electrochemical behaviour of the material at the single particle was confronted to the one at the composite level, which is influenced by the presence of conductive additives and polymeric binder.

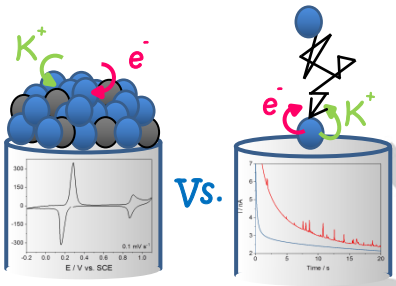

*Giorgia Zampardi, Stanislav V. Sokolov, Christopher Batchelor-McAuley and Richard G. Compton**

Page No. – Page No.

Potassium (De-)insertion Processes in Prussian Blue Particles: Ensemble versus Single Nanoparticle Behaviour